Available online at www.sciencedirect.com
ScienceDirect
Journal of Power Sources 175 (2008) 564–569
JOURNAL OF POWER SOURCES
www.elsevier.com/locate/jpowsour

Short communication

Morphology and electrochemical performance of $Li[Ni_{1/3}Co_{1/3}Mn_{1/3}]O_2$ cathode material by a slurry spray drying method

Bin Lin [a,b], Zhaoyin Wen [a,b,*], Zhonghua Gu [a], Shahua Huang [a,b]

[a] *Shanghai Institute of Ceramics, Chinese Academy of Sciences, Shanghai 200050, PR China*
[b] *Graduate School, Chinese Academy of sciences, 1295 DingXi Road, Shanghai 200050, PR China*

Received 20 June 2007; received in revised form 14 September 2007; accepted 19 September 2007
Available online 22 September 2007

Abstract

The spherical $Li[Ni_{1/3}Co_{1/3}Mn_{1/3}]O_2$ powders with appropriate porosity, small particle size and good particle size distribution were successfully prepared by a slurry spray drying method. The $Li[Ni_{1/3}Co_{1/3}Mn_{1/3}]O_2$ powders were characterized by XRD, SEM, ICP, BET, EIS and galvanostatic charge/discharge testing. The material calcined at 950 °C had the best electrochemical performance. Its initial discharge capacity was 188.9 mAh g^{-1} at the discharge rate of 0.2 C (32 mA g^{-1}), and retained 91.4% of the capacity on going from 0.2 to 4 C rate. From the EIS result, it was found that the favorable electrochemical performance of the $Li[Ni_{1/3}Co_{1/3}Mn_{1/3}]O_2$ cathode material was primarily attributed to the particular morphology formed by the spray drying process which was favorable for the charge transfer during the deintercalation and intercalation cycling.

Keywords: Lithium ion battery; $Li[Ni_{1/3}Co_{1/3}Mn_{1/3}]O_2$; Slurry spray drying; Spherical; Cathode material

1. Introduction

Extensive research has been carried out over past years to find alternative cathode materials to replace the presently popular $LiCoO_2$ for use in Li-ion battery. Recently, a layered transition metal oxide with hexagonal structure, $Li[Ni_{1/3}Co_{1/3}Mn_{1/3}]O_2$, was introduced by Ohzuku and Makimura as a candidate of cathode material to replace $LiCoO_2$ [1]. This material has attracted significant interests because of its many advantages such as higher reversible capacity with milder thermal stability at charged state [2], lower cost and less toxicity than $LiCoO_2$. Thus, $Li[Ni_{1/3}Co_{1/3}Mn_{1/3}]O_2$ might be one of the most promising candidates of cathode material for high-energy, high-power lithium-ion batteries [3]. As known, the performance of the powders used as cathode materials in lithium-ion batteries is strongly affected by their preparation processes [4]. Therefore, it is important to select a suitable method to prepare high performance $Li[Ni_{1/3}Co_{1/3}Mn_{1/3}]O_2$ [5].

$Li[Ni_{1/3}Co_{1/3}Mn_{1/3}]O_2$ was first prepared by conventional solid-state reaction method [1,6]. However, such method requires prolonged heat treatment at relatively high temperature with repeated intermediate grinding because of the heterogeneity of the precursors. In order to overcome these disadvantages, various new techniques, such as glycine-nitrate combustion [7], hydroxide co-precipitation [8–10], carbonate co-precipitation [11–13], ultrasonic spray pyrolysis [14], solution spray drying [4], sol–gel [15] process, etc., have been developed and applied to prepare high quality $Li[Ni_{1/3}Co_{1/3}Mn_{1/3}]O_2$. They lead to homogeneous materials with small particle size but these complex synthetic routes based on solution precursors require expensive initial or intermediate reagents, long time to dry the precursor. Moreover, the abundant use of organic acid or hydroxides, which are caustic to the production equipment, makes these methods not fit for the industrial-scale production for the materials.

Nakahara et al. [16] and Wen et al. [17] ever reported excellent electrochemical performance of particulate $Li_4Ti_5O_{12}$ prepared by slurry spray drying process with LiOH or Li_2CO_3 and TiO_2 as precursors. Different from the solution spray drying mentioned above, the slurry spray drying process uses the insoluble carbonates or oxides as precursor without any caustic reagents. The rapid heat and mass transfer occurring during the drying

* Corresponding author at: Shanghai Institute of Ceramics, Chinese Academy of Sciences, Shanghai 200050, PR China. Tel.: +86 21 52411704; fax: +86 21 52413903.
E-mail address: zywen@mail.sic.ac.cn (Z. Wen).

0378-7753/$ – see front matter © 2007 Elsevier B.V. All rights reserved.
doi:10.1016/j.jpowsour.2007.09.055

process result in dried granules having a large variety of shapes, i.e., from uniform solid spheres to elongated, pancake, donut-shaped, needlelike or hollow granules [18]. And the morphology has important effect on cell's performance.

In this paper, porous and spherical $Li[Ni_{1/3}Co_{1/3}Mn_{1/3}]O_2$ powders were prepared by a slurry spray drying process with Li_2CO_3, NiO, Co_3O_4 and $MnCO_3$ as precursors and polyvinyl butyral (PVB) as forming agent of pores, which could overcome the disadvantages of the solid-state reaction and various solution-based techniques. Moreover, the cost of the slurry spray drying method was much lower than the chemical processes. The morphology of the precursor and $Li[Ni_{1/3}Co_{1/3}Mn_{1/3}]O_2$ powders were investigated. The electrochemical properties of $Li[Ni_{1/3}Co_{1/3}Mn_{1/3}]O_2$ powders as cathode materials were studied by means of charge–discharge tests and electrochemical impedance spectroscopy in half cells.

2. Experimental

The proper amounts of precursors Li_2CO_3, NiO, Co_3O_4 and $MnCO_3$ (10% excess Li was used to compensate possible Li loss during the calcination and sintering process) were mixed in alcohol solvent by rotary ball milling at a speed of 300 rpm for 2 h to form a slurry, then 6 wt.% PVB was added and dissolved in the slurry and mixed for another 1 h. Then, the slurry was spray-dried with a spray-drier (Niro 2108, Denmark, air inlet temperature was 150 °C). The dried spherical powders were heated at 900–1000 °C for 10 h in an alumina crucible.

For comparison, $Li[Ni_{1/3}Co_{1/3}Mn_{1/3}]O_2$ was also prepared using a conventional solid-state reaction method with the same reagents used above. The precursor was obtained simply by grinding stoichiometric amounts of Li_2CO_3, NiO, Co_3O_4 and $MnCO_3$ in the same way as they did for the slurry spray drying method. The calcining process was the same as above.

Powder X-ray diffraction (XRD, Rigaku RINT-2000) measurement using Cu Kα radiation was employed to identify the crystalline phase of the synthesized materials. The scan range was 10–80° with a scan step of 0.02° and a scan speed of 10° min^{-1}. The chemical composition of the synthesized materials was determined by an inductively coupled plasma spectrometer (ICP, IRIS Advantage 1000). Scanning electron microscope (SEM, JEOL JSM-6700F) was applied to observe the morphology and particle size of the synthesized materials. The specific surface area was analyzed by the BET method using a Micromeritics Tristar 3000 in which the N_2 gas adsorption was employed. Each sample was heated to 150 °C for 4 h to remove any adsorbed water before the measurement.

The electrochemical performance of $Li[Ni_{1/3}Co_{1/3}Mn_{1/3}]O_2$ powders was evaluated with coin-type cells (CR 2025) using a lithium foil counter electrode and an electrolyte consisting of a 1 M $LiPF_6$ solution in EC:DMC (1:1, v/v) at room temperature. Microporous polypropylene membrane (Celgard) was used as the separator. The working electrode was prepared from a paste of 80 wt.% $Li[Ni_{1/3}Co_{1/3}Mn_{1/3}]O_2$ with 10 wt.% conductive acetylene black and 10 wt.% PVDF binder in NMP solvent. The paste was then coated on an aluminum foil, and finally dried under vacuum at 100 °C for 10 h before electrochemical evaluation. The battery was assembled in a glove box (VAC AM-2) filled with pure argon. All the cells were allowed to age for 10 h before testing. The galvanostatic charge–discharge tests were conducted on a LANDCT2001A battery test system with the cut-off voltages of 2.5 and 4.5 V (versus Li/Li^+) under a specific current density (a nominal specific capacity of 160 mAh g^{-1} was assumed to convert the current density into *C* rate). The electrochemical impedance spectroscopy (EIS) analysis was performed using a CHI760C Electrochemical Workstation over the frequency range from 0.1 MHz to 1 mHz with the amplitude of 5 mV.

3. Results and discussion

3.1. Phase analysis

Fig. 1 showed the XRD patterns of $Li[Ni_{1/3}Co_{1/3}Mn_{1/3}]O_2$ compounds prepared by both slurry spray drying and solid-state reaction method at 900–1000 °C, which were referred as SD900, SD950, SD1000 and SSR900, SSR950, SSR1000, respectively, where SD and SSR indicating spray drying and solid-state reaction, and the number indicating the treating temperature. As shown, the pure phase $Li[Ni_{1/3}Co_{1/3}Mn_{1/3}]O_2$ was obtained by solid-state reaction only at the calcining temperature above 950 °C. However, with regard to the slurry spray drying method, the pure phase could be obtained at the temperature as low as 900 °C. As can be seen in Fig. 1, regardless of calcination temperature, the intensity ratio of the (0 0 3)/(1 0 4) diffraction lines was higher than 1.2, indicating a low degree of cation mixing in the structure. The significant peak splitting of (0 0 6)/(1 0 2) and (1 0 8)/(1 1 0) could be observed in the XRD patterns for slurry spray drying samples which was known to be an indicator of the layered structure like $LiCoO_2$ and $LiNiO_2$ [5,19]. The lattice parameters of SD1000 powder were $a = 2.859$ and $c = 14.228$ Å calculated by least square

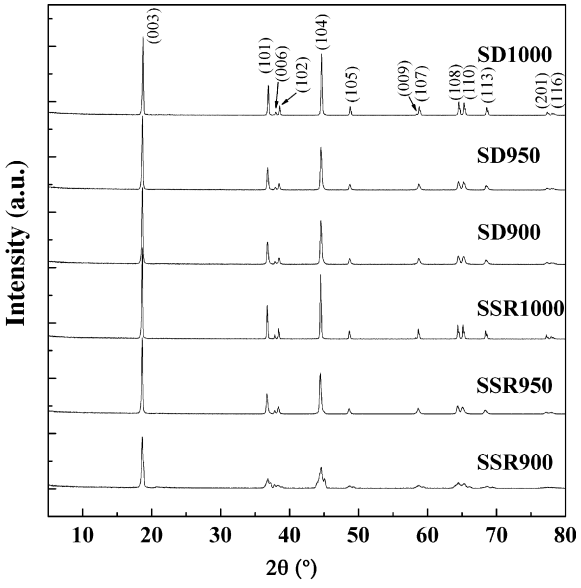

Fig. 1. XRD patterns of $Li[Ni_{1/3}Co_{1/3}Mn_{1/3}]O_2$ powders prepared by different methods.

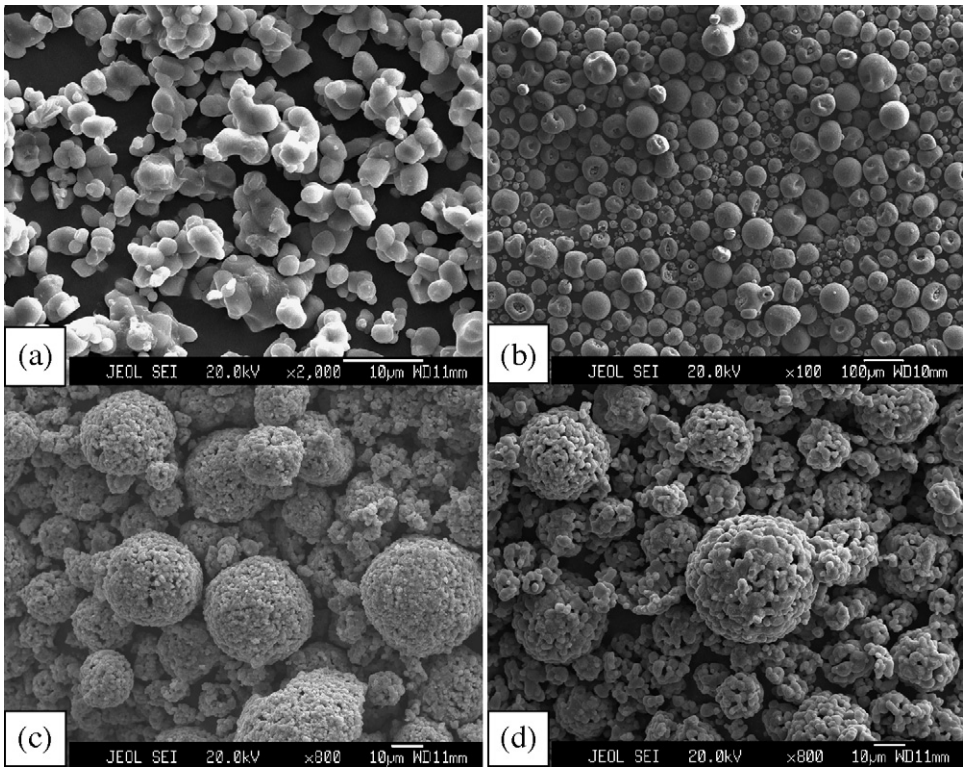

Fig. 2. SEM images of the powders: (a) $Li[Ni_{1/3}Co_{1/3}Mn_{1/3}]O_2$ powder by solid-state reaction method at 1000 °C, (b) the precursor by spray-dying method, and $Li[Ni_{1/3}Co_{1/3}Mn_{1/3}]O_2$ powder by spray drying method at 900 °C (c) and 1000 °C (d).

method using 10-diffraction lines, which were very close to those reported recently by Yabuuchi and Ohzuku [2]. The *c*/*a* ratio >4.97 also revealed the well-defined layered structure of the synthesized materials. The chemical composition of SD1000 was determined to be $Li_{1.01}Ni_{0.329}Co_{0.336}Mn_{0.335}O_2$, which was almost the same value as we designed. All the above results indicated that although the cations such as Li, Ni, Co and Mn were not distributed at an atomic level like the chemical processes such as sol–gel and hydroxide co-precipitation method, etc., the highly ordered $Li[Ni_{1/3}Co_{1/3}Mn_{1/3}]O_2$ was successfully obtained at lower temperature by the slurry spray drying process.

3.2. Morphological feature

Fig. 2 showed the morphology of the spray-dried precursor powders and the $Li[Ni_{1/3}Co_{1/3}Mn_{1/3}]O_2$ powders calcined at 900 and 1000 °C for 10 h, respectively. As shown in Fig. 2a, the material prepared by solid-state reaction method became hard-agglomerated from 2 to 40 μm, and was less uniform than that by spray-drying method. Its specific surface area was 2.1 $m^2\,g^{-1}$. With regard to the spray-dried sample, the particles were spherical and uniform with size of about 40 μm. It was seen that after calcining, the spherical particles shrank to about 30 μm and pores were formed after the decomposition of PVB binder. Its specific surface area was 3.9 $m^2\,g^{-1}$, nearly twice as large as that of SSR sample. The porous feature of the calcined spheres was helpful to the penetration of the liquid electrolyte and even the conducting agent carbon during the preparation of cathode. Fig. 2c and d showed the crystalline grains of SD900 and SD1000. It was observed that each large spherical particle was composed of such small ~1 μm particles, and the different calcining temperature resulted in different grain size and different discharge capacities as shown afterwards.

3.3. Cycling performance

Fig. 3 showed the initial charge/discharge curves of the different samples between 4.5 and 2.5 V with a current density of 32 mA g^{-1}. As seen, all the curves were very smooth and monotonous which was similar to the voltage profiles reported by other researchers [14,20]. The initial

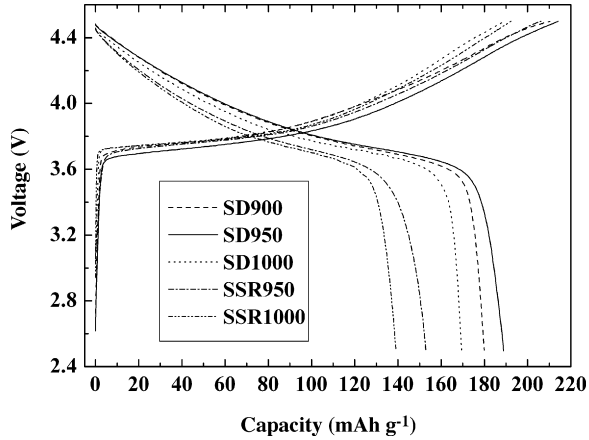

Fig. 3. Initial charge/discharge profiles of various $Li[Ni_{1/3}Co_{1/3}Mn_{1/3}]O_2$ powders at the discharge rate of 0.2 C in the potential range of 2.5–4.5 V.

charge/discharge capacity at room temperature was 206.3/152.9, and 192.4/139.1 mAh g^{-1} for SSR950 and SSR1000 samples, respectively, which was comparable to capacity (155 mAh g^{-1}) observed from other group by solid-state reaction method [4]. However, the SD900, SD950 and SD1000 samples displayed initial charge/discharge capacities of 210.4/179.9, 214.1/188.9 and 188.2/169.4 mAh g^{-1}, respectively. Much higher discharge capacity and lower irreversible capacity than those of the SSR samples were therefore obtained. This might be attributed to the less cation mixing property in the layer oxide cathode material prepared by slurry spray drying method [23].

Besides the differences in the capacity, the discharge profiles of the five samples had visible diversity. At the same discharge capacity, the discharge voltages of SD samples were higher than the SSR electrode. This meant that, the drawbacks of serious hysteresis voltage during the charge/discharge process of the $Li[Ni_{1/3}Co_{1/3}Mn_{1/3}]O_2$ powders prepared by conventional solid-state reaction method were effectively overcome by the slurry spray drying technique. Firstly, the granulating process of spray drying limited the excessive agglomeration of the grains, and the growing of the grains themselves. The smaller grain size resulted in a shorter diffusion path for Li^+ ions. Secondly, the porous structure led to great specific surface area, which was favorable to the permeation of the electrolyte. Thirdly, ordering the primary particles to larger entities by granulation formed a higher number of contacts between the primary particles during spray drying. Based on the above features, we expected the slurry spray drying process could improve the rate capability of $Li[Ni_{1/3}Co_{1/3}Mn_{1/3}]O_2$.

3.4. Rate properties

Fig. 4 showed the cycling performances of samples SD900, SD950, SD1000 and SSR950 at different rates. The cells were first charged at 0.10 mA cm^{-2} (32 mA g^{-1}, 0.2 C) until the voltage reached 4.5 V and then discharged at 0.10 mA cm^{-2} (32 mA g^{-1}, 0.2 C), 0.26 mA cm^{-2} (80 mA g^{-1}, 0.5 C), 0.52 mA cm^{-2} (160 mA g^{-1}, 1 C), 1.0 mA cm^{-2} (320 mA g^{-1}, 2 C) and 2.1 mA cm^{-2} (640 mA g^{-1}, 4 C) for every five cycles. As observed in Fig. 4, the discharge capacities gradually decreased with increasing current density. The SSR950 sample retained only 70.6% of the capacity on going from 0.2 C (0.10 mA cm^{-2}) to 4 C (2.1 mA cm^{-2}) rate. However, SD samples showed much better capacity retention at high rates than SSR950. Particularly, the SD900 sample presented a capacity of 168.1 mAh g^{-1} at current density of 2.1 mA cm^{-2}, corresponding to 93.1% of its capacity at 0.10 mA cm^{-2}, showing the best rate capability among all the samples, and this was superior to the rate capability obtained from other solution methods [10,14]. This enhanced discharge capability at accelerated rates clearly demonstrated the advantages of the slurry spray drying method.

Fig. 5 compared the 2nd, 7th, 12th, 17th and 22nd charge–discharge curves of the four samples at the discharge rates of 0.2 C, 0.5 C, 1 C, 2 C and 4 C, respectively. As seen, the SD samples exhibited smaller IR drops between charge and discharge in the whole voltage range than the SSR950. And as the calcining temperature increased, the IR drops of the SD samples grew, which was in agreement with the result of rate experiment. Thus, it was suggested that the porous morphology, or the high specific surface area of the active materials produced by the slurry spray drying method played positive role in improving the performance of the electrode and therefore the lithium ion batteries.

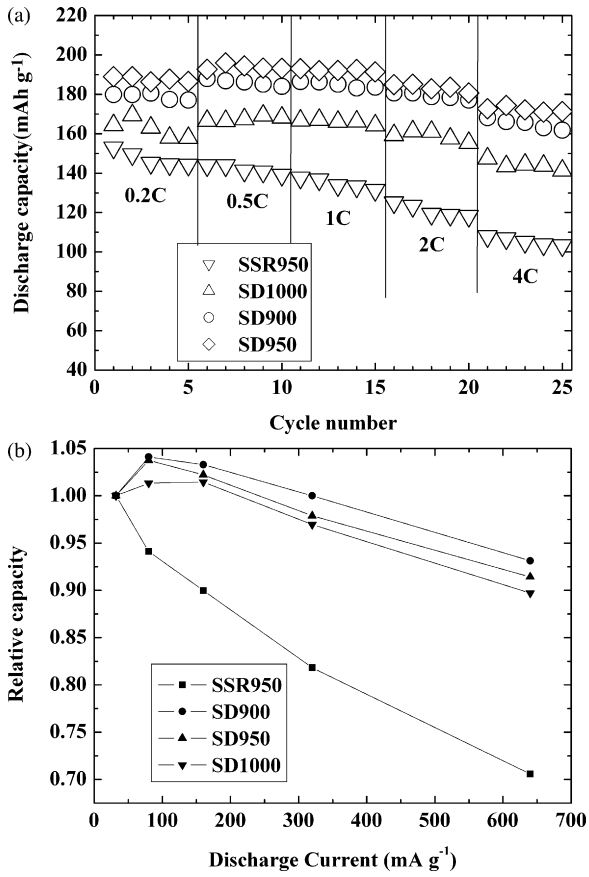

Fig. 4. Discharge capacity as a function of cycle number for $Li[Ni_{1/3}Co_{1/3}Mn_{1/3}]O_2$ powders at different current densities.

3.5. Impedance spectroscopy

To further understand the reason for the improved rate capability of $Li[Ni_{1/3}Co_{1/3}Mn_{1/3}]O_2$ prepared by slurry spray drying method, electrochemical impedance spectroscopy (EIS) was carried out for the SSR950 and SD950 samples at different cycle numbers in the charged state to 4.5 V versus Li/Li^+. In order to keep all samples at the same charge state, both the cells were first charged at constant current to 4.5 V and then followed by constant voltage charge (held at 4.5 V) for 10 h before the ac impedance data were collected. Nyquist plots of SSR950 and SD950 cells at the 5th cycle were shown in Fig. 6. The Nyquist plots for both electrodes presented two semicircles, one in the high-to-medium frequency region and the other in the low frequency region. According to Chowdari's and Sun's discussion concerning the electrochemical impedance spectroscopy of $Li[Ni_{1/3}Co_{1/3}Mn_{1/3}]O_2$ [21,22], the low frequency semicircle was normally considered as contributed from

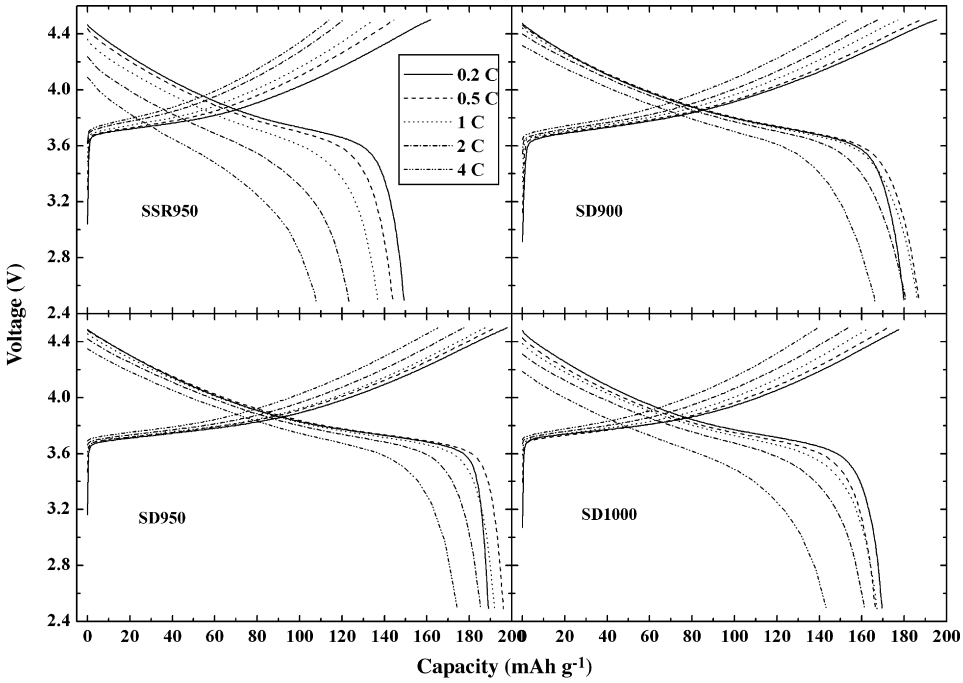

Fig. 5. Rate capability of Li/Li[$Ni_{1/3}Co_{1/3}Mn_{1/3}$]O_2.

the charge-transfer process (R_{ct}), and the high frequency contribution arose from the Li-ion migration through surface films that covers cathode particles (R_{sf}). As seen, the R_{sf} value of SD950 electrode was increased little comparing to the SSR950 electrode, because of its larger specific surface area. However, the charge-transfer resistance decreased drastically from 770 Ω of SSR950 sample to 62 Ω of SD950 sample. And the cell impendence was mainly attributed to charge-transfer resistance. It was therefore implied that the special morphology produced by the spray drying method would increase the contact surface between the electrolyte and electrode, and formed a higher number of contacts between the primary particles, which was of benefit to charge transfer, and hence decrease the kinetic resistance of the cell, as shown in Fig. 6. This was the reason that slurry spray drying method could improve the rate capability of Li[$Ni_{1/3}Co_{1/3}Mn_{1/3}$]O_2.

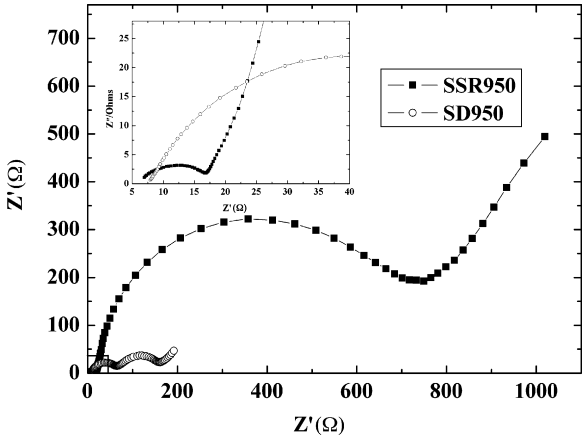

Fig. 6. Nyquist plots of SSR950 and SD950 electrode at 5th cycle.

4. Conclusion

The spherical Li[$Ni_{1/3}Co_{1/3}Mn_{1/3}$]O_2 powders with appropriate porosity and good size distribution were prepared by a slurry spray-drying method. Although the same low cost raw materials as for solid-state reaction method were used in this preparation process, the electrochemical performance of the products was comparable or even superior to that of the popular hydroxide co-precipitation method, such as the high rate capability [10,14]. And this is one of the most important requirements established for the hybrid electric vehicle application. The material calcined at 950 °C had the best electrochemical performance. Its initial discharge capacity was 188.9 mAh g^{-1} at the discharge rate of 0.2 C, and retained 91.4% of the capacity on going from 0.2 to 4 C rate. The EIS results showed that the favorable electrochemical performance of the Li[$Ni_{1/3}Co_{1/3}Mn_{1/3}$]O_2 cathode material was primarily attributed to the particular morphology formed by the spray drying process which was favorable for the charge transfer during the deintercalation and intercalation cycling. On the whole, the simple and low-cost slurry spray drying method would be a promising technique to be applied in the industrial-scale production of the cathode materials for lithium ion batteries.

Acknowledgments

This work was financially supported by key project of Natural Science Foundation of China (NSFC) No. 20333040.

References

[1] T. Ohzuku, Y. Makimura, Chem. Lett. 30 (2001) 642.
[2] N. Yabuuchi, T. Ohzuku, J. Power Sources 119–121 (2003) 171.

[3] I. Belharouak, Y.K. Sun, J. Liu, K. Amine, J. Power Sources 123 (2003) 247.
[4] D.C. Li, T. Muta, L.Q. Zhang, M. Yoshio, H. Noguchi, J. Power Sources 132 (2004) 150.
[5] K.M. Shaju, G.V. Subba Rao, B.V.R. Chowdari, Electrochim. Acta 48 (2002) 145.
[6] J.M. Kim, H.T. Chung, Electrochim. Acta 49 (2004) 937.
[7] S. Patoux, M.M. Doeff, Electrochem. Commun. 6 (2004) 767.
[8] M.H. Lee, Y.J. Kang, S.T. Myung, Y.K. Sun, Electrochim. Acta 50 (2004) 939.
[9] S.T. Myung, G.H. Kim, Y.K. Sun, Chem. Lett. 33 (2004) 1388.
[10] J. Choi, A. Manthiram, Electrochem. Solid-Sate Lett. 7 (2004) A365.
[11] T.H. Cho, S.M. Park, M. Yoshio, Chem. Lett. 33 (2004) 704.
[12] T.H. Cho, S.M. Park, M. Yoshio, T. Hirai, Y. Hideshima, J. Power Sources 142 (2005) 306.
[13] S.H. Park, H.S. Shin, S.T. Myung, C.S. Yoon, K. Amine, Y.K. Sun, Chem. Mater. 17 (2005) 6.
[14] S.H. Park, C.S. Yoon, S.G. Kang, H.S. Kim, S.I. Moon, Y.K. Sun, Electrochim. Acta 49 (2004) 557.
[15] B.J. Hwang, Y.W. Tsai, D. Carlier, G. Ceder, Chem. Mater. 15 (2003) 3676.
[16] K. Nakahara, R. Nakajima, T. Matsushima, H. Majima, J. Power Sources 117 (2003) 131.
[17] Z. Wen, Z. Gu, S. Huang, J. Yang, Z. Lin, O. Yamamoto, J. Power Sources 146 (2005) 670.
[18] H. Mahdjoub, P. Roy, C. Filiatre, G. Bertrand, C. Coddet, J. Eur. Ceram. Soc. 23 (2003) 1637.
[19] Y. Gao, M.V. Yakovleva, W.B. Ebner, Electrochem. Solid-Sate Lett. 1 (1998) 117.
[20] N. Yabuuchi, Y. Koyama, N. Nakayama, T. Ohzuku, J. Electrochem. Soc. 152 (2005) A1434.
[21] K.M. Shaju, G.V. Subba Rao, B.V.R. Chowdari, J. Electrochem. Soc. 151 (2004) A1332.
[22] Y.K. Sun, S.W. Cho, S.W. Lee, C.S. Yoon, K. Amine, J. Electrochem. Soc. 154 (2007) A168.
[23] J. Cho, G. Kim, H.S. Lim, J. Electrochem. Soc. 146 (1999) 3571.